

RAPID CALCULATION OF UNSTEADY AIRCRAFT LOADS

Jernej Drofelnik¹, Andrea Da Ronch², Daniel Kharlamov³ and Yan Sun⁴

¹ Research Fellow

Faculty of Engineering and the Environment, University of Southampton, Highfield Campus,
Southampton, SO17 1BJ, UK
J.Drofelnik@soton.ac.uk

² Lecturer

Faculty of Engineering and the Environment, University of Southampton, Highfield Campus,
Southampton, SO17 1BJ, UK
A.Da-Ronch@soton.ac.uk

³ PhD Student

Faculty of Engineering and the Environment, University of Southampton, Highfield Campus,
Southampton, SO17 1BJ, UK
D.Kharlamov@soton.ac.uk

⁴ Assistant professor

Faculty of Engineering and the Environment, University of Southampton, Highfield Campus,
Southampton, SO17 1BJ, UK / State Key Laboratory of Aerodynamics, China Aerodynamics
Research and Development Center, Mianyang City, Sichuan, China
Y.Sun@soton.ac.uk / Yanskla@mail.ustc.edu.cn

Key words: Multi-fidelity aerodynamic flow solver, Rapid CFD methods, Unsteady flow problems.

Abstract. An efficient multi-fidelity aerodynamic solver for unsteady flow problems, combining the unsteady vortex lattice method and Navier–Stokes solver for the infinite-swept wing problem, is presented. The new flow solver is able to correctly reproduce the loads of the three-dimensional Navier–Stokes unsteady, non-linear loads around a representative wing configuration, at a computational cost of a two-dimensional Navier–Stokes computation. Numerical details of the unsteady vortex lattice method solver, developed for this purpose, and its verification are presented. The coupling algorithm of multi-fidelity solver is described, followed by its demonstration around swept-wing configurations. It is demonstrated that the newly developed framework reproduces the loads of a three-dimensional unsteady Navier–Stokes computation, with the speed-up up to 290-times for the same accuracy.

1 INTRODUCTION

At the early stages of the aircraft design process, a large parameter space is explored, where the designers are typically relying on empirical and linear correlations [1]. Several low-fidelity methods based on potential-flow theory exist for rapid estimation of unsteady aerodynamic loads, e.g. doublet lattice method (DLM). Main advantages of these techniques are, a) their high computational speed; b) straightforward set-up of the problem, using simplified descriptions of lifting surfaces; and c) their applicability, as the methods have been calibrated on a number of existing aircraft configurations to account for un-modeled nonlinear flow phenomena. Their main drawback is that they heavily rely on the existence and availability of previous data, and this hinders their applicability to the design of radically new configurations. On the contrary, high-fidelity methods based on the three-dimensional (3D) unsteady Reynolds-averaged Navier-Stokes (URANS) solvers provide a good alternative to existing practice, however, they are yet too expensive for routine use from the industrial viewpoint. Due to these reasons, there is the need for a medium-fidelity approach, which combines: a) consistency, the approach adheres to a sound physical and theoretical model, combining favorable elements of the low and of the high-fidelity approaches; b) conformity, the approach is able to predict effectively within the bounds of the high-fidelity approach, making every possible effort to keep the CPU costs limited; c) convenience, the approach introduces as little as possible modifications to the existing design process. Medium-fidelity approach offers the possibility to limit the risk of setting the target design loads already at early design phase. If target loads are underestimated, an expensive re-design is typically required. Equally, if the target loads are overestimated, the aircraft will be heavier than needed, with degraded performances [2].

For steady aerodynamics, several attempts have been made in the past to couple linear methods with nonlinear viscous lift slope of sectional airfoils. The algorithms were based either on correction of the circulation, Γ , [3, 4] or on the α -based correction method, [5, 6]. Most recently, Gallay and Laurendeau extended the α -based coupling algorithm [6] to general wings in steady subsonic and transonic flight regimes, and improved the aerodynamic load predictions at high angle-of-attacks [7, 8]. On the contrary, for unsteady aerodynamics, there is a lack of studies which couple unsteady linear methods with the nonlinear counterpart. Parenteau et al. [9] recently demonstrated two unsteady α -based coupling algorithms. The first one uses two-dimensional (2D) sectional viscous lift curve data in combination with quasi-unsteady corrections. Such algorithm is, however, limited to motions with small reduced frequencies and low angle-of-attacks. The second one uses an unsteady 2D URANS sectional lift curve database in combination with UVLM. Unfortunately, this approach has its limitations, since the flow unsteadiness resolved by the 2D URANS approach is pre-computed, i.e. unsteady and dynamic flow effects are treated in the usual way commonly adopted for flight mechanics aerodynamic tables, by employing dynamic derivatives [10, 11].

With the above paragraphs as background, the present work aims at making progress in rapid unsteady load calculations, with the development, implementation, and demonstra-

tion of an unsteady multi-fidelity aerodynamic solver. To this goal, we have previously demonstrated the 2D URANS solver for the infinite-swept wing (ISW) problem, implemented in the DLR-Tau code, herein after referred to as 2.5D+ solver, but only used standalone [12]. This limitation is removed here, where the generalization of the 2.5D+ solver within the unsteady multi-fidelity aerodynamic solver is discussed for the first time. The innovative aspects of the proposed work include the multi-fidelity unsteady solver, which couples in real-time, in-house built UVLM solver, based on Katz and Plotkin formulation [13], and 2.5D+ URANS solver [12]. The new solver may capture strongly non-linear finite-wing effects encountered near stall flow conditions around swept wings, at a computational cost of a 2D URANS computation. The unified analysis tool may be used for both low- and high-speed aerodynamic analyses. Imperative to the successful deployment of the multi-fidelity solver is the coupling algorithm, which is fully discussed in this paper. The solver builds on the latest advances in algorithmic solutions, which are significantly faster than current state-of-the-art solvers. The work presents a part of a larger project carried out at the University of Southampton to develop a rapid computationally efficient aerodynamic method suitable for preliminary sizing aircraft studies.

The novelty of the work is the development of an unsteady algorithm to allow calculations in the time domain without the usual restrictions of a pre-computed database. The strength of the method is a seamless integration within an industrial process, as discussed in [12]. To the best of the authors' knowledge, this is the first reported study on the multi-fidelity unsteady solver.

First, the description of methodology is given in section 2. UVLM solver is introduced in subsection 2.1. The proposed methodology of an unsteady multi-fidelity coupling algorithm builds upon an 2.5D+ solver described in subsection 2.2. The description of the multi-fidelity unsteady algorithm is presented in subsection 2.3. Section 3 demonstrates verification of the newly developed UVLM solver. Section 4 describes the transonic wing test case used to demonstrate multi-fidelity solver. Section 5 contains results for transonic unsteady flow problems. Lastly, conclusions are given.

2 METHODOLOGY

The proposed multi-fidelity solver builds upon the UVLM solver, to model 3D effects, and the 2.5D+ URANS solver, to capture the sectional viscous effects. These two solvers are coupled by a time-accurate scheme for unsteady analyses.

2.1 Unsteady vortex lattice method

The UVLM solver implementation follows the description given by Katz and Plotkin [13]. At the end of each time step, a new row of wake panels is shed with a vortex strength equal to its circulation of the trailing edge panel. The induced velocities are calculated with the Bio-Savart law and incorporated in the aerodynamic influence matrix. The influence of the wake is added to the right-hand side *RHS* vector.

The linear system of equations is solved for each collocation point K at each time step:

$$\sum_{L=1}^m a_{KL} \Gamma_L = RHS_K \quad (1)$$

where a_{KL} is the KL -th component of the aerodynamic influence matrix and RHS_K is the right-hand side vector of each collocation point K . If the shape of the wing does not change, the matrix inversion occurs only during the first time step.

Once the vortex distribution is obtained the pressures and loads are calculated. A non-planar formulation is used to estimate the loads using Kutta–Joukowski theorem [14].

2.2 Infinite-swept wing solver

The second flow solver employed in the multi-fidelity solver is the DLR–Tau flow solver [16], which is a finite volume based CFD computational framework used by a number of aerospace industries across Europe. Among several features, the flow solver contains a very efficient algorithm for solving the steady and unsteady, incompressible and compressible flow around an ISW, at computational cost of 2D URANS simulation. This specialized algorithm, known as 2.5D+ solver, was implemented by the authors in DLR–Tau version 2016.1.0 [15] and is now used for production. The influence of the wing sweep angle within the context of a purely 2D grid stencil is dealt with imposing appropriate boundary conditions at the far-field. More details about the algorithm, boundary conditions, and application on a variety of test cases are found in [12]. The 2.5D+ solver is a key capability for the work presented in this study, as it can account for the cross-flow effects, required by the multi-fidelity solver.

2.3 Multi-fidelity solver

The sketch of proposed approach is depicted in Fig. 1. The spanwise position and number of URANS sections is a user given choice. The multi-fidelity solver is based on the α -based coupling algorithm [13], which corrects the freestream angle-of-attack at every panel using the nonlinear sectional data of the URANS solver. Imperative to the successful deployment of the multi-fidelity solver is the coupling algorithm, which allows calculations in the time domain without the usual restrictions of a pre-computed non-linear database.

The coupling algorithm is depicted in Fig. 2. The first step is to initialize the UVLM and URANS solvers. At each physical time-step, the equations of these solvers are advanced in pseudo-time, and information exchanged using the α -based coupling algorithm. Once the solution is converged, it is then used for the next physical time-step. Within the α -based coupling algorithm, there is a nested inner loop, which requires convergence of the UVLM and URANS lift coefficients, below the tolerance level ϵ . The nested inner loop consists of two main operations: i) solve the linear system of UVLM equations (Eq. 1) to obtain the UVLM lift coefficient C_L^{UVLM} and the induced angle-of-attack α_i , which is required for the estimation of the effective angle-of-attack:

$$\alpha_{eff} = \alpha_\infty - \alpha_i \quad (2)$$

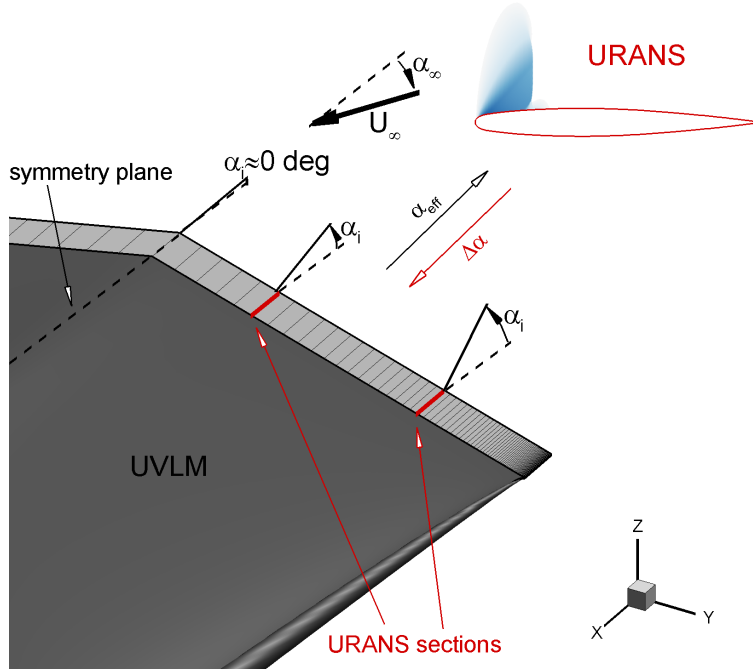


Figure 1: Schematics of an unsteady multi-fidelity coupling algorithm UVLM + 2D URANS.

where α_∞ denotes the freestream angle-of-attack; ii) run a limited number of URANS inner iterations at α_{eff} to obtain the URANS lift coefficient C_L^{UVLM} , which is required for the estimation of the angle-of-attack correction:

$$\Delta\alpha = \nu \frac{C_L^{URANS} - C_L^{UVLM}}{2\pi} \quad (3)$$

where ν represents the relaxation factor, to make the iterative procedure more stable. It is worth noting that C_L^{URANS} and C_L^{UVLM} are function of the time step, the instantaneous

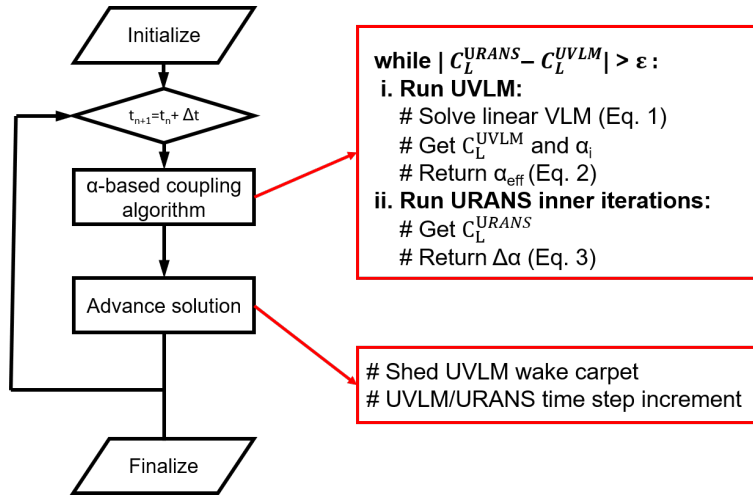


Figure 2: Unsteady mixed-fidelity coupling algorithm UVLM + 2D URANS.

angle-of-attack and its derivative. For brevity, these dependencies are omitted from the notation. Once $\Delta\alpha$ has been estimated, α_∞ is adjusted at every panel; if the user selects more than one URANS section, linear interpolations of $\Delta\alpha$ are performed across the span. This completes one cycle of the nested inner loop. The iterative loop continues until convergence of the lift coefficient is achieved. Advancing of the solution includes shedding of the wake carpet behind the wing, and the increment of the physical time of both UVLM and URANS solvers. Once the solution becomes periodic, the time dependent loop is completed. Lastly, the computation is finalized, and memory is deallocated.

The coupling algorithm, which synchronizes the execution of the UVLM and URANS solvers, is written in Python. By using the Python C-API, data is continuously exchanged between Python and C subroutines of the UVLM code. A Python wrapper of the DLR-Tau code is also employed, which allows to call subroutines of the URANS solver directly from the main framework and exchange data over shared memory. This avoids more time consuming exchange procedures of data between the codes using the file system.

3 VERIFICATION OF UVLM

3.1 Steady planar wings

At first the validation of the inviscid steady solution of VLM against experimental data from [13] is performed. Figure 3 depicts the lift coefficient slope, computed for the planar wings of various sweep angles, Λ , and aspect ratios, AR . To assure convergence of all cases, 8 panels have been used in chordwise ($N_x = 8$), and 26 panels in spanwise ($N_y = 26$) directions. The experimental and numerical data are in excellent agreement.

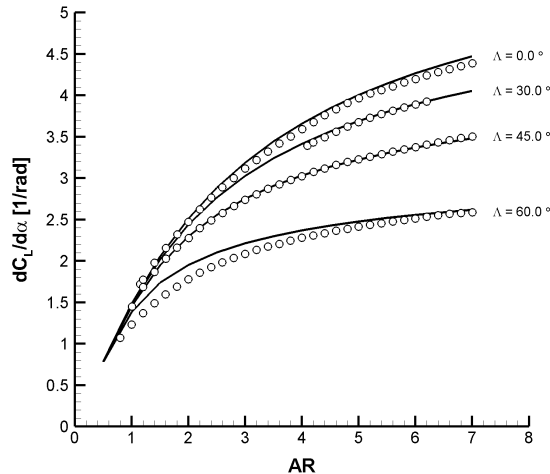


Figure 3: Steady lift coefficient slope for a flat plate with different aspect ratios and sweep angles ($N_x = 8$, $N_y = 26$).

3.2 Aerofoil in pitching motion

The predicting capabilities of the UVLM solver have been demonstrated for a pitching motion of a thin airfoil by comparison with the unsteady, incompressible, irrotational 2D solution from Theodorsen [17]. Analytical solution exists for a thin airfoil undergoing small harmonic oscillations in a uniform free stream. The representation of a 2D airfoil in UVLM solver was obtained by using the large aspect ratio of the wing, $AR = 100$, in combination with coarse spanwise distribution, which implies that 3D effects are ignored. Pitching motion is given by the following expression, respectively:

$$\alpha_\infty(t) = \alpha_0 + \alpha_A \sin(2k\tau) \tag{4}$$

where α_0 is the mean angle-of-attack, and α_A is the pitching amplitude. The symbol k denotes the reduced frequency $k = \omega c/2U_\infty$, and τ is the non-dimensional time.

UVLM results are compared with the analytical solution of Theodorsen, at three different reduced frequencies, $k = 0.25, 0.5$ and 0.75 . α_0 was set to 0 deg and $\alpha_A = 2$ deg. The number of chordwise panels has been adjusted for each reduced frequency, with the relation $N_x = 56 \times k$, as suggested in [18]. The number of spanwise panels was set to $N_y = 12$. The wake roll-up function was disabled. Furthermore, we have followed the suggestion in [18], that the relationship between the non-dimensional time step used in the calculation is as follows: $\Delta\tau = \frac{1}{N_x}$.

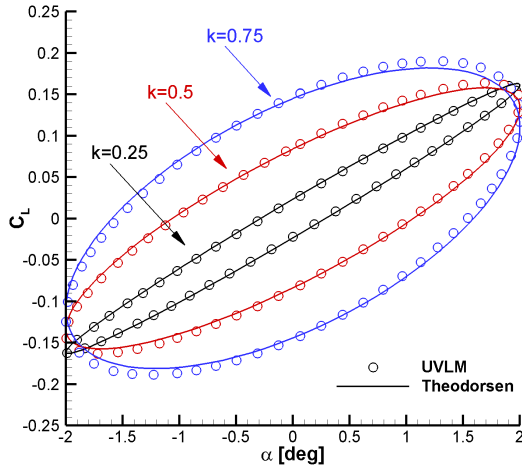


Figure 4: Lift coefficient of an infinite wing undergoing harmonic pitch oscillations at three different reduced frequencies ($N_x = 56 \times k$, $N_y = 12$, $\Delta\tau = \frac{1}{N_x}$).

Figure 4 represents the harmonic pitch oscillations of a thin airfoil. For all cases three oscillation cycles are computed, to assure periodic solution, and the initial transient was removed from the comparison. The UVLM results are in excellent agreement with Theodorsen’s analytical solution for all reduced frequencies, which confirms the correctness of implementation.

4 TEST CASE

4.1 Forced Sinusoidal Motion of wing

The test case to demonstrate multi-fidelity solver concerns transonic flow predictions around a wing undergoing a forced sinusoidal motion in pitch, given by the Eq. 4. The flow conditions are for $M_\infty = 0.755$ and $Re_\infty = 5.5 \cdot 10^6$. The motion is characterized by a reduced frequency $k = 0.0814$, mean angle of attack $\alpha_0 = 0.016$ deg and amplitude $\alpha_A = 2.51$ deg. Since there is a lack of experimental data for a 3D wings undergoing forced motion in transonic flow, we have adapted the well-known 2D AGARD CT 5 configuration, pitching at one-quarter of the chord. The flow field presents the formation of a strong and highly dynamic shock wave, the steady solution includes a virtually symmetric shock wave which periodically appears and disappears on the upper and lower surfaces as consequence of the harmonic motion. A fairly large $AR = 20$ wings, using the NACA 0012 aerofoil, have been constructed for three different sweep angles.

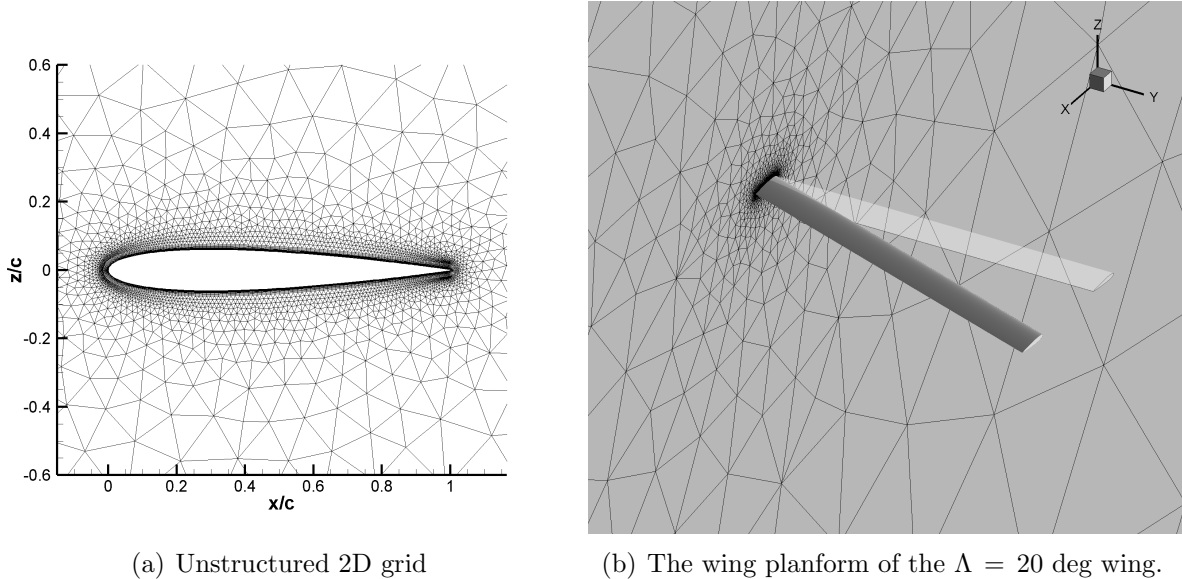


Figure 5: Grids for the transonic NACA 0012 wing.

Four sets of grids were used for the analyses. The unstructured 2D grid, depicted in Fig. 5, was employed to solve the 2D and 2.5D+ URANS equations. The grid consists of about 15.3 thousand mesh elements with the first layer on the wall at $5 \cdot 10^{-6}$ (for a chord of one), ensuring $y^+ < 1$. Furthermore, for the dependence of the wing sweep angle ($\Lambda = 0, 10, 20$ deg) on the aerodynamic loads, three finite-span $AR = 20$ wings were built by stacking the 2D unstructured grid in the spanwise direction from the midspan symmetry plane to the lateral farfield boundary. Fig. 5(b) depicts the 3D grid with the sweep angle of $\Lambda = 20$ deg. For all cases 128 points have been used in spanwise direction, featuring about 2 million mesh elements, and a symmetry boundary condition was enforced at midspan, to halve the computational cost. The Spalart–Allmaras (SA) turbulence model and an implicit dual-time stepping scheme were employed, with a target

residual drop of three orders at each physical time step. For the multi-fidelity solver a target residual drop of three orders at each time step is also enforced.

5 RESULTS

5.1 Forced sinusoidal motion of NACA0012 wing

For all cases, the UVLM and URANS solvers started from the freestream initial conditions. All solvers used 100 physical time steps per oscillating cycle. In the figures below, URANS is referring to the solvers of DLR-Tau code, and URANS + UVLM is referring to multi-fidelity solver, described in section 2.3. Pure UVLM solution is not included, because it is invalid at this transonic flow regime, or it would need compressibility correction based on the semi-empirical approach of Prandtl-Glauert. We chose, instead, to show how the multi-fidelity solver can overcome these two problems implicitly.

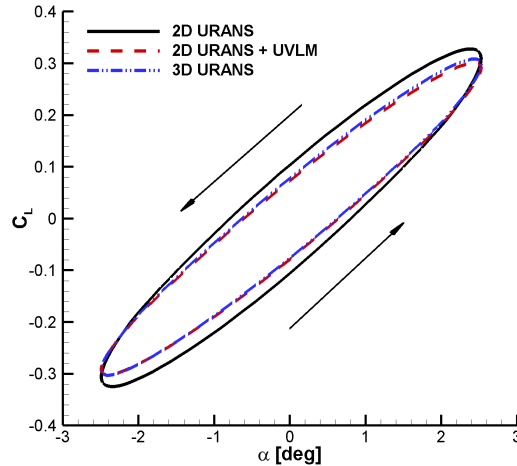


Figure 6: Lift coefficient dependence on forced sinusoidal motion for sweep angle $\Lambda = 0$ deg ($M_\infty = 0.755$, $Re_\infty = 5.5 \cdot 10^6$, $k = 0.0814$, $\alpha_0 = 0.016$ deg, $\alpha_A = 2.51$ deg).

Figure 6 shows the comparison of the lift coefficient for sweep angle $\Lambda = 0$ deg for the increased fidelity levels. For the multi fidelity solver, $N_x = 1$, $N_y = 50$ and only one section at midspan was corrected with the URANS calculation. One may notice there is an excellent agreement between the multi-fidelity and 3D URANS solutions. The 3D effects are well captured with the UVLM solver, and the solution is well corrected with the 2D URANS. The 2D URANS solution can clearly not capture the 3D effects, although of limited extent for this wing, and is visibly different from other two solutions.

Figure 7(a) shows the comparison of the lift coefficient for sweep angle $\Lambda = 10$ deg, for the increased fidelity levels. For the multi fidelity solver, $N_x = 1$, $N_y = 50$ and only one section at 20% semi-span was corrected with the 2D or 2.5D+ URANS calculations. Again, there is an excellent agreement between the multi-fidelity solver based on 2.5D+ URANS correction and 3D URANS solution. The solution of the UVLM solver is well

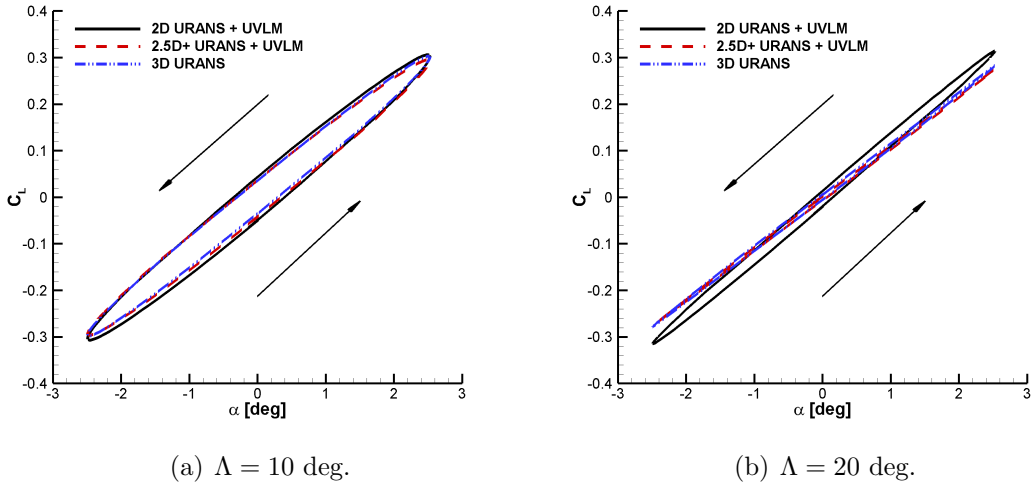


Figure 7: Lift coefficient dependence on forced sinusoidal motion for two sweep angles ($M_\infty = 0.755$, $Re_\infty = 5.5 \cdot 10^6$, $k = 0.0814$, $\alpha_0 = 0.016$ deg, $\alpha_A = 2.51$ deg).

corrected with the 2.5D+ URANS solution. The multi-fidelity solver based on 2D URANS correction does not agree well with other two solutions, since the 2D URANS can not capture the cross-flow effects.

Finally, Fig. 7(b) shows the comparison of the lift coefficient for sweep angle $\Lambda = 20$ deg, for the increased fidelity levels. For the multi fidelity solver, $N_x = 1$, $N_y = 50$ and only one section at 20% semi-span was corrected with the 2D or 2.5D+ URANS calculations. Also for $\Lambda = 20$ deg, there is an excellent agreement between the multi-fidelity solver based on 2.5D+ URANS correction and 3D URANS solution. Here it is evident the necessity of the 2.5D+ solver since the solution of the multi-fidelity solver based on 2D URANS correction is incorrect, as the cross-flow effects are not accounted in the solution.

The multi-fidelity solver provides a physically consistent solution of aerodynamic loads, in comparison to that obtained from a 3D solution but at a fraction of the computational time. Specifically, 146 CPU hours per oscillatory cycle were needed for the calculation around the 3D wing. The CPU time per cycle was reduced to about 30 minutes when employing the multi-fidelity approach, which corresponds to a speed-up of about 290 compared to the 3D URANS analysis.

6 CONCLUSIONS

An efficient multi-fidelity solver was discussed, which combines the unsteady vortex lattice method solver, capturing 3D effects, with the infinite-swept wing unsteady Navier-Stokes solver, reproducing the sectional viscous effects. The solver is based on the α -based coupling algorithm, which corrects the freestream angle-of-attack at every panel using the nonlinear sectional data of the unsteady Navier-Stokes solver. The strong point of the new solver is the coupling algorithm, which allows calculations in the time domain

without the usual restrictions of a pre-computed non-linear database. The proposed solver was thoroughly validated against numerical data obtained from 3D Navier–Stokes solution.

Two main conclusions may be formulated. The first is that the proposed method retains the same accuracy of calculating the aerodynamic loads of the full 3D unsteady Navier–Stokes solution. The second conclusion regards the extremely high efficiency of the proposed method. The multi-fidelity solver retains a computational cost of a 2D unsteady Navier–Stokes computation, thus, the speed-up of 290 of the proposed method against the 3D Navier–Stokes solution has been obtained.

ACKNOWLEDGMENTS

Da Ronch and Drofelnik gratefully acknowledge the financial support from the Engineering and Physical Sciences Research Council (grant number: EP/P006795/1). Mr M. Cross and Mr T. Engelbrecht of Airbus Operation Limited are acknowledged for their assistance and comments on industrial practice.

REFERENCES

- [1] Rizzi, A. Modeling and simulating aircraft stability and control – The SimSAC project, *Progress in Aerospace Sciences* (2011) **47(8)**:573–588.
- [2] Butchers, M. Uncertainty quantification & management in high value manufacturing special interest group, *Annual Report, The Knowledge Transfer Network* (2015).
- [3] Tani, I. *A simple method of calculating the induced velocity of a monoplane wing*. Aeronautical Research Institute, Tokyo Imperial University, 1934.
- [4] Multhopp, H, and Schwabe, M. *Die Berechnung der Auftriebsverteilung von Tragflügeln*, 1938.
- [5] Tseng, J.B. and Lan, C.E. *Calculation of aerodynamic characteristics of airplane configurations at high angles of attack*, NASA-CR-4182, 1988.
- [6] Van Dam, C.P. and Vander Kam, J.C. and Paris, J.K. Design-oriented high-lift methodology for general aviation and civil transport aircraft, *Journal of aircraft* (2001) **38(6)**:1076–1084.
- [7] Gallay, S. and Laurendeau, E. Nonlinear Generalized Lifting-Line Coupling Algorithms for Pre/Poststall Flows, *AIAA Journal* (2015) **53(7)**:1784–1792.
- [8] Gallay, S and Laurendeau, E. Preliminary-Design Aerodynamic Model for Complex Configurations Using Lifting-Line Coupling Algorithm, (2016) **53(4)**:1145–1159.
- [9] Parenteau, M. and Plante, F. and Laurendeau, E. and Costes, M. Unsteady Coupling Algorithm for Lifting-Line Methods, *55th AIAA Aerospace Sciences Meeting* (2017) AIAA 2017–0951.

- [10] Da Ronch, A. and Ghoreyshi, M. and Badcock, K. On the generation of flight dynamics aerodynamic tables by computational fluid dynamics, *Progress in Aerospace Sciences* (2011) **47(8)**:597–620.
- [11] Da Ronch, A. and Vallespin, D. and Ghoreyshi, M. and Badcock, K. Evaluation of dynamic derivatives using computational fluid dynamics, *AIAA Journal* (2012) **50(2)**:470–484.
- [12] Franciolini, M. and Da Ronch, A. and Drofelnik, J. and Raveh, D. and Crivellini, A. Efficient Infinite-swept Wing Solver for Steady and Unsteady Compressible Flows, *Aerospace Science and Technology* (2018) **72**:217–229.
- [13] Katz, J. and Plotkin, A. *Low-speed aerodynamics*. Cambridge University Press, 2001.
- [14] Simpson, R. and Palacios, R. and Murua, J. Induced-Drag Calculations in the Unsteady Vortex Lattice Method, *AIAA Journal* (2013) **51(7)**: 101–144.
- [15] Droffenik, J. and Da Ronch, A. 2.5D+ User Guide. Documentation for DLR-Tau flow solver, 2017.
- [16] Schwamborn, D. and Gerhold, T. and Heinrich, R. The DLR TAU-code: recent applications in research and industry, *Proceedings of the European Conference on Computational Fluid Dynamics (ECCOMAS)*, 2006.
- [17] Theodorsen, T. and Mutchler, W.H. *General theory of aerodynamic instability and the mechanism of flutter*. National Advisory Committee for Aeronautics Washington, DC, USA, 1935.
- [18] Murua, J. Flexible aircraft dynamics with a geometrically-nonlinear description of the unsteady aerodynamics. Doctoral thesis, Imperial College London, 2012.